Pergamon

0277-5387(95)00104-2

Polyhedron Vol. 14, No. 20–21, pp. 3041–3050, 1995

0277-5387/95 $9.50+0.00

SYNTHESIS, SPECTROSCOPIC AND ELECTROCHEMICAL PROPERTIES OF TETRAZOLATOMANGANESE(III) PORPHYRINS

R. GUILARD,† N. JAGÉROVIC and J.-M. BARBE

Laboratoire d'Ingénierie Moléculaire pour la Séparation et les Applications des Gaz, "LIMSAG" (UMR 9953), University of Bourgogne, Faculté des Sciences "Gabriel", 6 Boulevard Gabriel, 21100 Dijon, France

and

Y. H. LIU, I. PERROT, C. NAILLON, E. VAN CAEMELBECKE and K. M. KADISH†

Department of Chemistry, University of Houston, Houston, TX 77204-5641, U.S.A.

(*Received* 6 *December* 1994; *accepted* 24 *February* 1995)

Abstract—The synthesis, spectroscopic characterization and electrochemical properties of four tetrazolatomanganese(III) porphyrins are reported. The investigated compounds are represented by (TPP)Mn[$N_4C(R)$], where TPP is the dianion of tetraphenylporphyrin and R is CH_2CH_3, C_6H_5, CH=CH_2 or CH=CHCN. Each complex was characterized by IR, UV–vis and ^1H NMR spectroscopy, as well as by mass spectrometry. Variable-temperature ^1H NMR data demonstrate that the electron-withdrawing effect of the tetrazolato ligand in (TPP)Mn[$N_4C(R)$] is higher than that of the azido axial ligand in (TPP)MnN_3. The reductions of each σ-bonded (TPP)Mn[$N_4C(R)$] derivative were also examined in four non-aqueous solvents (dichloromethane, benzonitrile, tetrahydrofuran and pyridine) and the resulting data compared with data in the literature for manganese(III) porphyrins containing an ionic axial ligand such as Cl^- or ClO_4^-.

Manganese porphyrins have long been studied as model compounds for tetrapyrrole-containing enzymes which are involved in several biological processes.[1–7] More recently they have been used for DNA cleavage[8] and could also be considered as potential contrast enhancement agents for magnetic resonance imaging.[9] The metal ion in synthetic manganese porphyrins can exist in a large number of oxidation states and this is of interest with respect to the particular chemical reactivity and catalytic properties of the compounds.[10]

The most studied synthetic manganese porphyrins are those with anionic axial ligands, although compounds with other types of axial ligands have been characterized.[5,7–10] No studies of σ-bonded manganese porphyrins have yet appeared in the literature and in the present paper we describe the first synthesis, spectroscopic characterization and electrochemical properties of four Mn^{III} σ-bonded tetrazolato derivatives. These compounds were synthesized using the known reaction of azido organic compounds with organic nitriles[11–15] and provide a series of compounds for comparison with previously synthesized indium(III),[16] iron(III),[17] germanium(IV)[18] and tin(IV)[18] porphyrins containing σ-bonded tetrazolato axial ligands.

The compounds described in the present study are represented by (TPP)Mn[$N_4C(R)$], where TPP is the dianion of tetraphenylporphyrin and R is CH_2CH_3, C_6H_5, CH=CH_2 or CH=CHCN. Each Mn^{III} porphyrin was characterized by IR, UV–vis

†Authors to whom correspondence should be addressed.

and ^{1}H NMR spectroscopy, as well as by mass spectrometry after which its redox properties were examined in four non-aqueous solvents (dichloromethane, benzonitrile, tetrahydrofuran and pyridine). Variable-temperature ^{1}H NMR data demonstrate that the electron-withdrawing effect of the tetrazolato ligand in (TPP)Mn[$N_4C(R)$] is higher than that of the azido axial ligand in (TPP)MnN_3. The redox properties of each σ-bonded (TPP)Mn[$N_4C(R)$] derivative are compared with data in the literature for manganese(III) porphyrins containing an ionic axial ligand such as Cl^- or ClO_4^-.

EXPERIMENTAL

Chemicals

The synthesis and preparation of each tetrazolato complex was carried out under an argon atmosphere with common solvents being distilled under argon and thoroughly dried prior to use. All synthetic operations were carried out in Schlenk tubes. Propionitrile (CH_3CH_2CN), benzonitrile (C_6H_5CN) and acrylonitrile (CH_2=CHCN) were freshly distilled under an inert atmosphere. Fumaronitrile (CNCH=CHCN) was used without further purification. Methylene chloride (CH_2Cl_2) was distilled over P_2O_5. Tetra-n-butylammonium perchlorate [(TBA)ClO_4] was purchased from Fluka Corp. and twice recrystallized, first from absolute ethanol and then from ethylacetate, after which it was dried in a vacuum oven at 40°C.

Preparation of the compounds

The starting (TPP)MnN_3 derivative used in the synthesis of (TPP)Mn[$N_4C(R)$] was synthesized from (TPP)MnCl and sodium azide (NaN_3), as described in the literature.[17] The four tetrazolato complexes were synthesized by one of two different methods depending upon the R group. The first method involves a direct reaction of (TPP)MnN_3 with the nitrile (propionitrile or benzonitrile) which was used as the solvent, while the second involves addition of the nitrile to toluene solutions of (TPP)MnN_3 as described below. Yields and recrystallization solvents are given in Table 1. Two different synthetic pathways were used to obtain (TPP)Mn[$N_4C(R)$] derivatives and are detailed below.

(TPP)Mn[$N_4C(C_2H_5)$]. A solution of (TPP)MnN_3 (0.46 g, 0.65 mmol) in propionitrile (60 cm^3) was refluxed for 24 h. The solvent was then evaporated *in vacuo* and the resulting solid recrystallized in a toluene/heptane mixture (2.5/1) to give 0.18 g of the final product (yield = 37%). MS [(*m*/*z*) ab. %]: 764 $(M)^+$, 4; 667 $[M-N_4C(C_2H_5)]^+$, 100.

(TPP)Mn[$N_4C(C_6H_5)$]. The same method was used with benzonitrile and gave (TPP)Mn[$N_4C(C_6H_5)$] in 31% yield. MS [(*m*/*z*) ab. %]: 813 $(M+H)^+$, 1; 667 $[M-N_4C(C_2H_5)]^+$, 100.

(TPP)Mn[N_4C(CH=CHCN)]. The same method was used for the synthesis of (TPP)Mn[$N_4C(CH{=}CH_2)$]. To a solution of 0.20 g of (TPP)MnN_3 (0.28 mmol) in toluene (30 cm^3) was added fumaronitrile (0.04 g, 0.77 mmol) to give the (TPP)Mn[N_4C(CH=CHCN)] derivative after refluxing for 13 h. The solvent was then evaporated *in vacuo* and the resulting solid tetrazolato complex recrystallized in a toluene/heptane (5/1) mixture (0.17 g, yield = 77%). MS [(*m*/*z*) ab. %]: 787 $(M)^+$, 2; 667 $[M-N_4C(C_2H_5)]^+$, 100.

(TPP)Mn[$N_4C(CH{=}CH_2)$]. The same method was used with benzonitrile and gave (TPP)Mn[$N_4C(CH{=}CH_2)$] in 56% yield. 760 $(M-2H)^+$, 2; 667 $[M-N_4C(C_2H_5)]^+$, 100.

Instrumentation

^{1}H NMR spectra were recorded at 400 MHz on a Bruker WM 400 spectrometer of the "Centre de Spectrométrie Moléculaire de l'Université de Bour-

Table 1. Elemental analyses, yields and solvents utilized for recrystallization of (TPP)Mn[$N_4C(R)$]

Axial ligand	Recrystallization solvent[a]	Yield[b] (%)	Molecular formula	Analyses[c] % C	% H	% Mn	% N
$N_4C(CH_2CH_3)$	A	37	$C_{47}H_{33}N_8Mn$	73.5 (73.8)	4.4 (4.4)	6.9 (7.2)	14.0 (14.6)
$N_4C(C_6H_5)$	A	31	$C_{51}H_{33}N_8Mn$	74.3 (75.4)	4.3 (4.1)	6.6 (6.7)	13.2 (13.8)
$N_4C(CH{=}CH_2)$	B	56	$C_{47}H_{31}N_8Mn$	68.2 (74.0)	4.8 (4.1)	4.2 (7.2)	18.8 (14.7)
N_4C(CH=CHCN)	C	77	$C_{48}H_{30}N_9Mn$	73.8 (73.2)	4.0 (3.9)	6.2 (7.0)	14.2 (16.0)

[a] A = toluene/heptane (2.5/1), B = toluene, C = toluene/heptane (5/1).
[b] Yield after recrystallization.
[c] Calculated values given in parentheses.

gogne". Spectra were measured with 5 mg of the investigated complex in deuterated solvents and tetramethylsilane was used as the internal reference. Mass spectra were recorded on a Kratos Concept 32S of the "Centre de Spectrométrie Moléculaire de l'Université de Bourgogne" in the DCI mode (NH_3 as the reagent gas). IR spectra were obtained on a Perkin–Elmer 580 B apparatus. Solid samples were prepared as a 1% dispersion in CsI. Electronic absorption spectra were recorded on a Perkin–Elmer 559 spectrophotometer, an IBM Model 9430 spectrophotometer or a Tracor Northern 6500 spectrometer. ESR spectra were recorded on an IBM Model ER-100D electron spin resonance system.

Cyclic voltammograms were obtained using a three-electrode system. The working electrode was a platinum button, the counter electrode a platinum wire and the reference electrode a saturated calomel electrode (SCE) which was separated from the bulk of the solution by a fritted-glass bridge.

RESULTS AND DISCUSSION

Synthesis

The conversion of (TPP)MnN_3 to (TPP)Mn[$N_4C(R)$] proceeds as shown in eq. (1) and was monitored spectroscopically by following the disappearance of the ν_{N-N} vibration in the IR spectrum of the starting compound. The resulting (TPP)Mn[$N_4C(R)$] complexes more easily hydrolyse than the corresponding indium(III) derivatives[16] and result in the generation of hydroxo derivatives of the type (TPP)Mn(OH).

$$(TPP)MnN_3 + RCN \longrightarrow (TPP)Mn[N_4C(R)] \quad (1)$$

The formation of the tetrazolato ring as shown in eq. (1) seems to depend upon the type of porphyrin ring and the specific organic nitrile as well as upon the porphyrin central metal ion. For example, (TPP)InN_3 reacts with acetonitrile[16] which is not the case for (TPP)MnN_3.

Spectral characterization of (TPP)Mn[$N_4C(R)$]

Elemental analyses, yields and recrystallization solvents for the formation of each five-coordinate (TPP)Mn[$N_4C(R)$] derivative are given in Table 1. The elemental analyses are in good agreement with the proposed molecular formulae for three of the four synthesized compounds, the only exception being (TPP)Mn[$N_4C(CH{=}CH_2)$]. However, as shown in the following paragraphs, a comparison of the physicochemical data on this derivative with previously reported data for the (TPP)In[$N_4C(CH{=}CH_2)$][16] unambiguously proves the assigned molecular formula.

Mass spectral data obtained by desorption chemical ionization (DCI) were used in conjunction with several spectroscopic techniques to characterize each neutral complex. Each spectrum shows either the molecular ion or a pseudo-molecular ion, which confirms the formula as (TPP)Mn[$N_4C(R)$]. The parent peak corresponds to the $[(TPP)Mn]^+$ moiety for all four compounds and this illustrates the facile cleavage of the manganese–tetrazolato bond, as is also the case for the metal–nitrogen bond in (P)In[$N_4C(R)$][16] and (P)Fe[$N_4C(R)$][17] where P is one of several different porphyrin macrocycles.

Characteristic IR bands of the investigated compounds are summarized in Table 2. Each metalloporphyrin, except (TPP)Mn[$N_4C(CH{=}CH_2)$], exhibits absorption peaks located between 1000 and 1455 cm^{-1} which are associated with the vibration of the tetrazolato ring.[14] The vibrational frequencies listed in Table 2 are also in good agreement with results reported earlier for tetrazolato porphyrin complexes containing indium(III),[16] iron(III),[17] tin(IV)[18] or germanium(IV)[18] central metal ions.

Vibrational frequencies for the aryl, alkyl or alkene groups of the tetrazolato ring of (TPP)Mn[$N_4C(R)$] are listed in Table 2 and were assigned by comparison with data in the literature for related compounds.[19] The vibration frequencies of the C=C and $CH{=}CH_2$ bonds in (TPP)Mn[$N_4C(CH{=}CHCN)$] and (TPP)Mn[$N_4C(CH{=}CH_2)$] are located at 1629 and 1650 cm^{-1},

Table 2. IR data for (TPP)Mn[$N_4C(R)$] in CsI pellets (ν cm^{-1})

Axial ligand	Vibrations of R group	Vibrations of tetrazolato ring
$N_4C(CH_2CH_3)$	2965, 2925, 2855	1408, 1055
$N_4C(C_6H_5)$		1455, 1360, 1115, 1035, 1000
$N_4C(CH{=}CH_2)$	3100, 2960, 1650, 990	
$N_4C(CH{=}CHCN)$	2218, 1629	1382, 1154

Table 3. UV–vis data for (TPP)Mn[$N_4C(R)$] and (TPP)MnN_3 in THF

Axial ligand	λ_{max}, nm ($\varepsilon \times 10^{-3}$)[a] Soret region				Q bands			
N_3^-	350 (86.7)	372 (85.3)	400 (70.3)	425 (47.6)	476 (97.3)	538 (4.5)	595 (4.7)	636 (7.7)
$N_4C(CH_2CH_3)$	355 (33.7)	378 (40.4)	400 (38.2)	432 (34.3)	478 (87.6)	529 (5.2)	581 (8.0)	619 (8.6)
$N_4C(C_6H_5)$	358 (34.1)	379 (43.4)	401 (42.7)	432 (25.4)	476 (90.7)	525 (5.4)	572 (8.4)	610 (8.7)
$N_4C(CH{=}CH_2)$	350 (63.3)	377 (62.0)	402 (52.9)	432 (40.7)	476 (78.1)	525 (12.5)	572 (13.6)	610 (10.8)
$N_4C(CH{=}CHCN)$	350 (61.8)	375 (56.3)	404 (47.9)	430 (30.0)	476 (80.0)	520 (4.9)	574 (5.8)	612 (5.1)

[a] ε ($M^{-1}\,cm^{-1}$).

respectively. The CH_2CH_3 group of (TPP)Mn[$N_4C(CH_2CH_3)$] exhibits both symmetrical and antisymmetrical CH_2 stretching bands and these are located at 2855 and 2925 cm^{-1}. The band at 2965 cm^{-1} is assigned to an antisymmetrical valence vibration of the methyl group. The 2218 cm^{-1} band of (TPP)Mn[$N_4C(CH{=}CHCN)$] corresponds to a vibration of the terminal C≡N group, but no vibrational peak is detected for the Mn—N(tetrazolato) bond.

UV–vis data of the four synthesized compounds are given in Table 3. The spectra are similar to those reported for five-coordinate manganese(III) tetraphenylporphyrins containing an anionic axial ligand such as Cl^-, ClO_4^- or N_3^-[21 24] and this might be taken as evidence for the anionic nature of the σ-bonded $N_4C(R)$ axial ligand. The Mn^{III} metal ion and the porphyrin π-ring system weakly interact with each other, and the UV–vis data in Table 3 are all characteristic of *d*-type hyperporphyrins.[20] These high-spin Mn^{III} complexes have a d^4 configuration and the lowest orbitals (d_{xy}, d_{xz} and d_{z^2}) are singly occupied. For this reason, several ligand-to-metal charge-transfer transitions are allowed and the UV–vis spectra can be interpreted in terms of $\pi \rightarrow \pi^*$ and macrocycle → metal charge-transfer transitions.

Boucher has assigned the six most prominent visible absorption bands of manganese(III) porphyrins[1] and similar spectra are obtained for the (TPP)Mn[$N_4C(R)$] derivatives which exhibit two bands in the visible region and are slightly blue shifted (2–26 nm) with respect to the position of the bands for the starting azido complex. However, no significant shift is observed in the Soret region of the spectrum and this suggests that the anionic character of the $N_4C(R)$ axial ligand in (TPP)Mn[$N_4C(R)$] is similar to that of Cl^-, ClO_4^- or N_3^-[21 24] when bound to the Mn^{III} centre of a (TPP)MnX complex.

^1H NMR data of the synthesized compounds are summarized in Table 4. The chemical shifts and the line-widths (10–1500 Hz) are characteristic of paramagnetic compounds and an assignment of the (TPP)Mn[$N_4C(R)$] resonances can be made by comparison with previously characterized manganese(III) porphyrins containing other axial ligands such as Cl^-, ClO_4^- or N_3^-.[21–24] The pyrrole-H signals of the TPP complexes appear as the broadest peaks (1500 Hz) in the ^1H NMR spectrum and are located between −28.9 and −38.4 ppm. Resonances for the *m*-H and *p*-H protons are seen at *ca* 8.0 and 7.2 ppm, respectively, but none of the *o*-H resonances are detected.

The proton resonances of the R group on the bound tetrazolato ring are difficult to assign. For example, signals are located between 7.50 and 8.30 ppm for (TPP)Mn[$N_4C(C_6H_5)$], but these cannot be unambigously attributed to the C_6H_5 protons due to a superposition of these signals with those of the non-deuterated solvent. On the other hand, proton resonances of the $CH{=}CH_2$ group in (TPP)Mn[$N_4C(CH{=}CH_2)$] are clearly seen in the NMR spectrum. As seen in Table 4, the $=CH_2$ protons of the $N_4C(CH{=}CH_2)$ moiety appear as a pair of doublets (at 6.11 and 6.00 ppm) which have a 24 Hz coupling constant. A broad signal of the CH= proton of this species is observed at 4.72 ppm and this resonance is similar to a value reported for the analogous (TPP)In[$N_4C(CH{=}CH_2)$] derivative under the same solution conditions[16] [see Fig. 1(a)].

The ^1H NMR spectrum of (TPP)Mn[$N_4C(CH{=}CH_2)$] was also recorded over the tem-

Table 4. ^{1}H NMR data (400 MHz) for (TPP)Mn[N_4C(R)] and (TPP)MnN_3[a]

Axial ligand	R^{1}[b]	R^{2}[b]	R[b]	Protons of R^1	Protons of R^2	Protons of R
N_3^-	C_6H_5	H		(*m*-H) 8.24 (*p*-H) 7.19	−23.1	
$N_4C(CH_2CH_3)$	C_6H_5	H	CH_2CH_3	(*m*-H) 8.20 (*p*-H) 7.18	−28.9	
$N_4C(C_6H_5)$	C_6H_5	H	C_6H_5	(*m*-H) 8.24 (*p*-H) 7.18	−30.0	
$N_4C(CH{=}CH_2)$	C_6H_5	H	$CH{=}CH_2$	(*m*-H) 8.20 (*p*-H) 7.20	−38.4	(vinyl H) 6.11 (d[b,c]) (vinyl H) 6.00 (d[b,c]) (vinyl H) 4.72 (M[b])
$N_4C(CH{=}CHCN)$	C_6H_5	H	$CH{=}CHCN$	(*m*-H) 8.15 (*p*-H) 7.18	−32.0	

[a] Spectra recorded in $CDCl_3$ at 294 K chemical shifts are given in ppm using $Si(CH_3)_4$ as an internal reference.

[b]

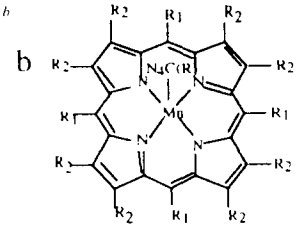

[c] d = doublet, M = unresolved multiplet.

[d] J = 24 Hz.

perature range 238–312 K in $CDCl_3$ in order to examine the correlation between isotropic shifts and temperature. The chemical shifts are referenced against those of (TPP)In[$N_4C(CH{=}CH_2)$] which is diamagnetic and isostructural. The isotropic chemical shifts, $(\Delta H/H)_{iso}$, for the protons of (TPP)Mn[N_4C(R)] are listed in Table 5 and the temperature dependence of chemical shifts for the pyrr-H and *m*-H resonances of [(TPP)Mn[$N_4C(CH{=}CH_2)$] are shown in Fig. 1(b). A linear dependence on T^{-1} is observed for the pyrr-H resonances, but not for the *m*-H resonances. Similar results have earlier been reported for manganese(III) porphyrins containing other axial ligands.[24,25]

Electron delocalization onto the tetrazolato ligand of [(TPP)Mn[N_4C(R)] is likely to change the contact interactions which exist between unpaired electrons of the Mn^{III} metal ion and protons of the porphyrin macrocycle. Indeed, it should be noted that shifts are observed between the proton resonances of the tetrazolato manganese porphyrins with respect to those of (TPP)MnN_3. These results unambiguously show that the tetrazolato ligand increases the contact interaction, a result which is in agreement with a higher electron-withdrawing effect of the σ-bonded tetrazolato axial ligand compared with the anionic azide axial ligand. This result is also reflected in $E_{1/2}$ values for the first reduction of the σ-bonded tetrazolato and azido complexes as discussed in the following section.

Table 5. Isotropic chemical shifts, $(\Delta H/H)_{iso}$,[a] for (TPP)Mn[N_4C(R)] in $CDCl_3$

Axial ligand	pyrr-H	*m*-H	*p*-H
$N_4C(CH{=}CH_2)$	−47.5	+0.4	−0.6
$N_4C(CH{=}CHCN)$	−41.1	+0.4	−0.6

[a] $(\Delta H/H)_{iso}$ given in ppm where the corresponding diamagnetic reference is (TPP)In[N_4C(R)].[15]

Electroreduction of (TPP)Mn[N_4C(R)]

The electroreduction of (TPP)Mn[N_4C(R)] was investigated in up to four different non-aqueous solvents, each containing 0.1 M (TBA)ClO_4. Half-wave potentials for the reductions are given in Table 6 and representative voltammograms for one of the compounds, (TPP)Mn[$N_4C(C_6H_5)$], are shown in Fig. 2. Similar reductive behaviour is obtained for the four investigated tetrazolato complexes in a given solvent. This is illustrated in Fig. 3 which shows voltammograms for reduction of each

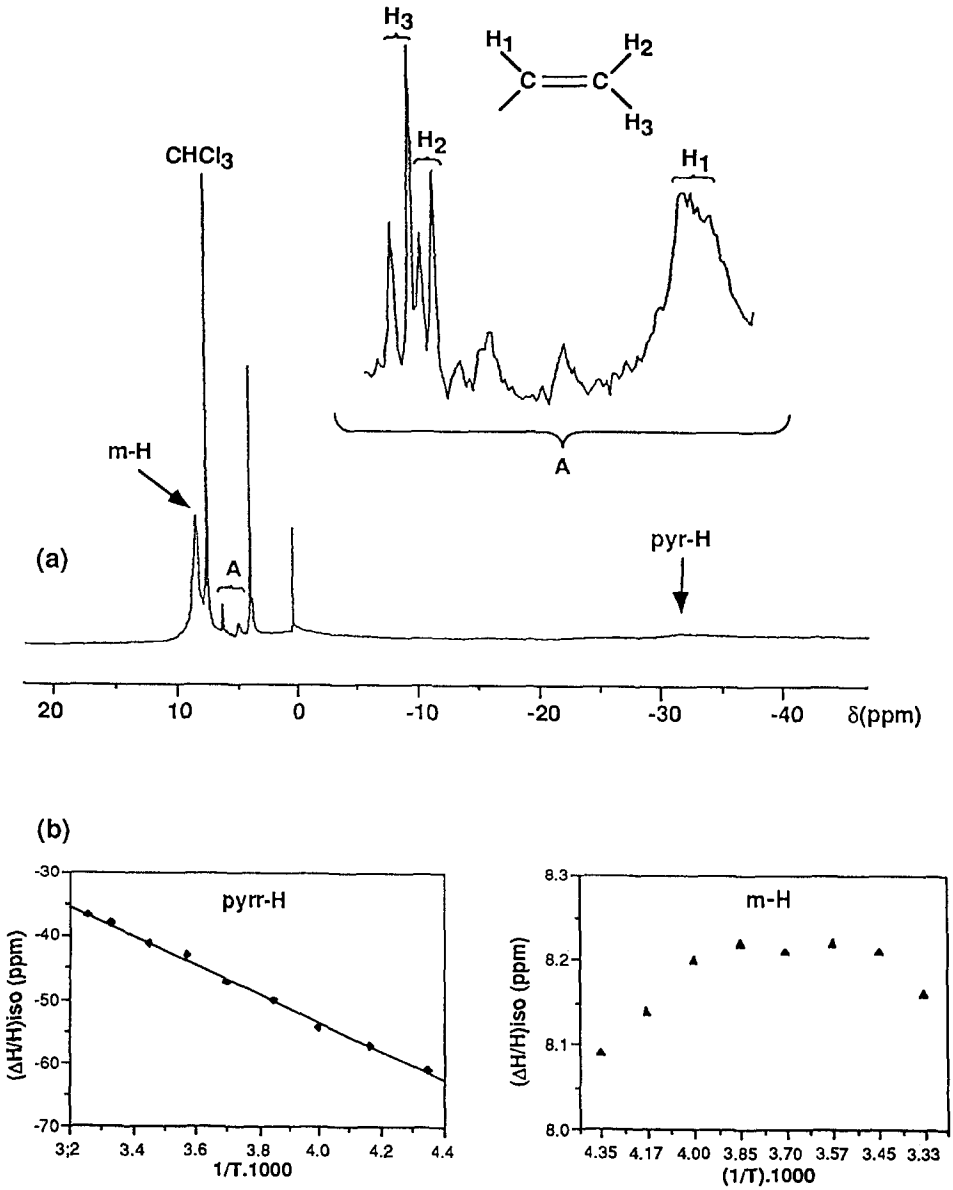

Fig. 1. (a) ^{1}H NMR spectrum and (b) temperature dependence for isotropic shifts of (TPP)Mn[$N_4C(CH{=}CH_2)$] in $CDCl_3$.

(TPP)Mn[$N_4C(R)$] derivative in CH_2Cl_2 containing 0.1 M (TBA)ClO_4.

The first reduction of (TPP)Mn[$N_4C(R)$] in CH_2Cl_2 occurs at $E_{1/2}$ values between -0.25 and -0.27 V and is characterized by a peak potential separation, $|E_{pa}-E_{pc}|$, of 100–140 mV for a potential scan rate of 0.1 V s^{-1}. These half-wave potentials are within the range of $E_{1/2}$ values reported for the first one-electron reduction of various Mn^{III} tetraphenylporphyrins containing anionic axial ligands[26-28] and can specifically be compared with $E_{1/2}$ values which fall in the range -0.25 to -0.29 V for the metal centred reductions of (TPP)MnSCN, (TPP)MnBr and (TPP)MnCl under the same experimental conditions.[27-28] The values for (TPP)Mn[$N_4C(R)$] can also be compared with an $E_{1/2}$ of -0.16 V for the reduction of (TPP)$MnClO_4$ and -0.34 V for the reduction of (TPP)MnN_3[27,28] in CH_2Cl_2, 0.1 M (TBA)ClO_4.

Time-resolved spectra which were recorded during the one-electron controlled potential reduction of (TPP)Mn[$N_4C(C_6H_5)$] at -0.50 V in CH_2Cl_2 0.2 M (TBA)ClO_4 are shown in Fig. 4. As the reaction proceeds, the Soret band at 485 nm decreases in intensity and disappears while a new band at 438 nm appears. At the same time, the two visible bands

Table 6. Reduction potentials of the investigated (TPP)Mn^{III} complexes in several solvents containing 0.1 M (TBA)ClO_4 as the supporting electrolyte

Ligand	Solvent	1st	2nd	3rd
ClO_4^- [a]	CH_2Cl_2	−0.16	−1.51	
	PhCN	−0.14	−1.34	
Cl^-	CH_2Cl_2	−0.29	−1.62[b]	
	PhCN	−0.24	−1.48	
	THF	−0.22	−1.30	−1.87[b]
	Py	−0.23	−1.32	−1.83
$N_4C(C_6H_5)$	CH_2Cl_2	−0.27	−1.62[b]	−1.80
	PhCN	−0.28	−1.39	
	THF	−0.23	−1.39	−1.98[b]
	Py	−0.23	−1.32	−1.83
$N_4C(C_2H_3)$	CH_2Cl_2	−0.25	−1.58[b]	
	PhCN	−0.26	−1.41	
	THF	−0.25	−1.29	−1.38
	Py	−0.23	−1.32	−1.83
$N_4C(C_3H_2N)$	CH_2Cl_2	−0.25	−1.60[b]	
	PhCN	−0.19	−1.40	
	THF	−0.26	−1.35	−2.06
	Py	−0.23	−1.32	−1.83
$N_4C(C_2H_5)$	CH_2Cl_2	−0.25	−1.50[b]	
	PhCN	−0.30	−1.43	

[a] Reference 29.
[b] E_{pc} value at 0.1 V s^{-1}.

shift respectively from 584 and 620 to 571 and 610 nm. Similar changes in the UV–vis spectra are seen for the other three investigated tetrazolato derivatives and the data are consistent with the conversion of (TPP)$Mn^{III}[N_4C(R)]$ to [(TPP)Mn^{II} $[N_4C(R)]]^-$.[29,30] The spectral changes shown in Fig. 4 are reversible and the spectrum of the original neutral compound could be fully regenerated upon controlled-potential oxidation at 0.0 V.

The site of electron transfer upon reduction of (TPP)Mn$[N_4C(R)]$ was also confirmed by ESR spectroscopy. Each electroreduced porphyrin is ESR active and the resulting spectral data are summarized in Table 7. The shape of the low-field six-line ^{55}Mn hyperfine pattern in the ESR spectrum of [(TPP)Mn^{II}[$(N_4C(R)]]^-$ indicates a g tensor with $g_\perp = 5.95$ to 6.05 and $g_\parallel = 1.95$ to 2.27 depending upon the specific $N_4C(R)$ axial ligand. The ^{55}Mn hyperfine interaction is isotropic with $A = 85$ G and the observed g values are typical of a high-spin d^5 system ($S = 5/2$).[30] As will be discussed in the following paragraphs, the electrogenerated [(TPP)Mn^{II}[$N_4C(R)]]^-$ derivatives seem to be sufficiently stable in CH_2Cl_2 so that a loss of the axial ligand does not occur on the cyclic voltammetry timescale. The ligand is, however, lost in a more strongly bonding solvent such as PhCN, THF or py, and this is reflected in the appearance of a third one-electron reduction which is best defined in pyridine as illustrated in Fig. 2.

Strong evidence for the binding of the $N_4C(R)$ ligand to the Mn^{II} centre of the singly reduced complex is given by the irreversible second reduction in CH_2Cl_2, which occurs at a peak potential that is shifted negatively by up to 300 mV compared with the same electrode reaction in a bonding solvent such as PhCN, THF or py (see Table 7).

Table 7. ESR data of singly reduced (TPP)Mn$[N_4C(R)]$ in CH_2Cl_2, 0.2 M (TBA)ClO_4 at 120 K

Axial ligand	$g_\perp$[a]	$g_\parallel$
$N_4C(C_6H_5)$	5.95 (85)	2.27
$N_4C(CH{=}CH_2)$	6.05 (86)	1.95
$N_4C(CH_2CH_3)$	6.02 (85)	2.10
$N_4C(CH{=}CHCN$	6.04 (85)	1.97

[a] Values in parentheses are coupling constants in Gauss.

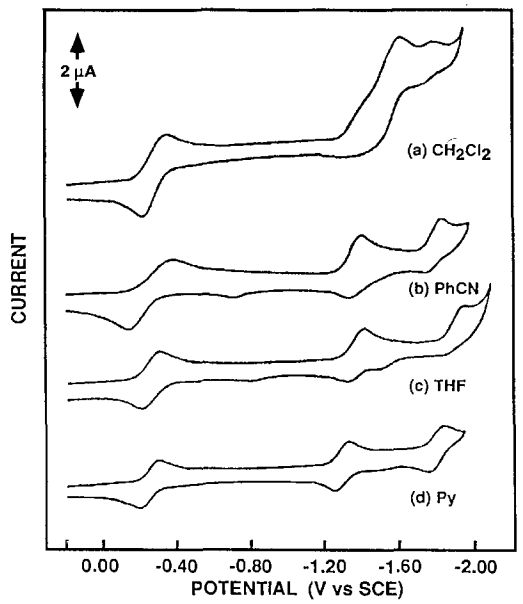

Fig. 2. Cyclic voltammograms of (TPP)Mn[$N_4C(C_6H_5)$] in (a) CH_2Cl_2, (b) PhCN, (c) THF and (d) py containing 0.1 M (TBA)ClO_4.

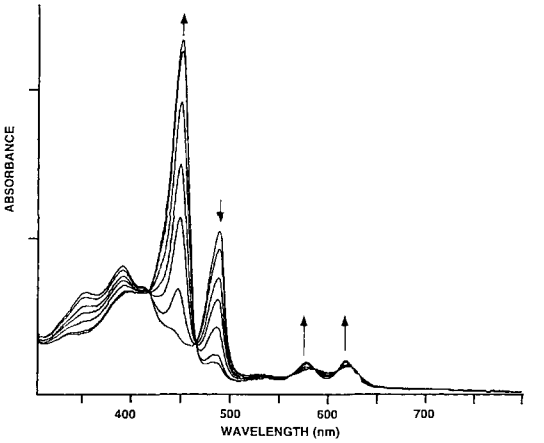

Fig. 4. Time-resolved electronic absorption spectra recorded during the controlled potential reduction of (TPP)Mn[$N_4C(C_6H_5)$] at −0.50 V in CH_2Cl_2, 0.2 M (TBA)ClO_4.

Electroreduction in pyridine or CH_2Cl_2/py *mixtures*

Fig. 5 shows cyclic voltammograms of (TPP)Mn[$N_4C(C_6H_5)$] in CH_2Cl_2 containing 0.1 M (TBA)ClO_4 before and after addition of pyridine to solution. As pyridine is progressively added, the second reductions located at $E_{1/2} = -1.62$ V in neat CH_2Cl_2 disappears and two new well-defined reductions begin to appear at $E_{1/2} = -1.38$ and -1.83 V. Neither of the new processes shift in potential upon further addition of pyridine and the electrode reactions may be assigned as the con-

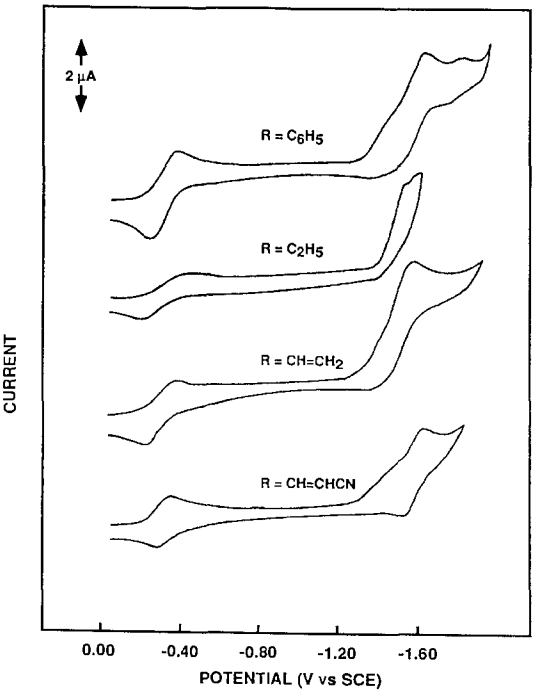

Fig. 3. Cyclic voltammograms showing the reduction of (TPP)Mn[$N_4C(R)$] in CH_2Cl_2 containing 0.1 M (TBA)ClO_4^-. Scan rate = 100 mV s^{-1}.

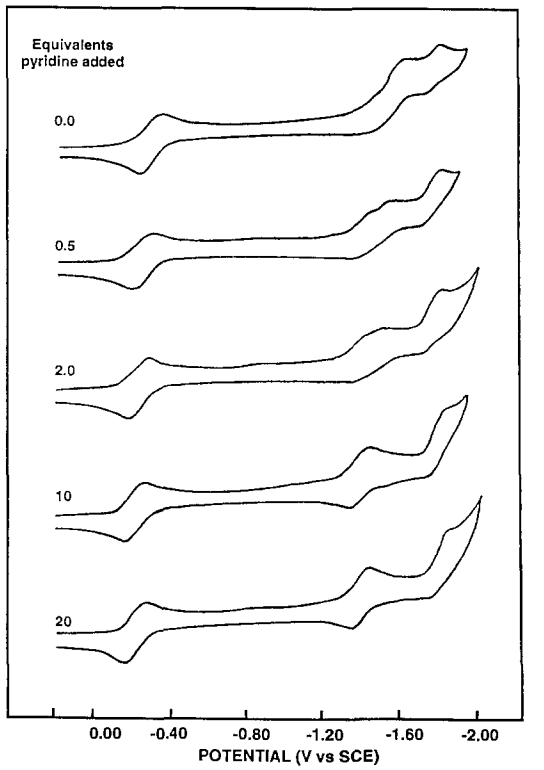

Fig. 5. Cyclic voltammogram showing the reduction of 1.0×10^{-3} M (TPP)Mn[$N_4C(C_6H_5)$] in CH_2Cl_2 solutions containing 0.1 M (TBA)ClO_4 and 0–20 equiv. of pyridine.

version of (TPP)Mn^{II}(py) to [(TPP)Mn^{II}(py)]$^-$ followed by the formation of a Mn^{II} porphyrin dianion.[28] The $E_{1/2}$ for the last two reductions of (TPP)Mn[$N_4C(C_6H_5)$] are similar to values for the other three (TPP)Mn[N_4C(R)] complexes in solutions containing 20 equiv. py and are also close to the $E_{1/2}$ values in neat pyridine (see Table 6). This implies that the same doubly and triply reduced species are present in solution under both experimental conditions.

The $E_{1/2}$ for the Mn^{III}/Mn^{II} reaction of (TPP)Mn[N_4C(R)] in the mixed-solvent system is shown in Fig. 6 as a function of py concentration. There is an anodic potential shift in $E_{1/2}$ with an increase in [py] from 10^{-3} to $\approx 8 \times 10^{-3}$ M (region II), but no shift at either lower or higher concentrations of pyridine (regions I and III). Furthermore, the magnitude of the slope in region II of Fig. 6 is -0.062 V and can be accounted for by the addition of one pyridine molecule to the Mn^{II} product of the (TPP)Mn[N_4C(R)] reduction. A similar figure has been presented in the literature for (TPP)MnCl in CH_2Cl_2/py mixtures[28] and was interpreted in terms of a loss of the Cl^- axial ligand accompanied by pyridine binding to the neutral and/or reduced porphyrin product, depending upon the concentration of pyridine in solution. Interestingly, $E_{1/2}$ for the first reduction of (TPP)MnCl in the CH_2Cl_2/py mixture becomes independent of the pyridine concentration after addition of 100 equiv. py and this can be compared to a similar result for (TPP)Mn[N_4C(R)] where the invariant $E_{1/2}$ is obtained after only 10 equiv. of pyridine have been added to solution. This implies that the Cl^- axial ligand binds more strongly to Mn^{III} than does [N_4C(R)]$^-$ which is also the conclusion resulting from a comparison of the (TPP)MnCl and (TPP)Mn[N_4C(R)] redox potentials.

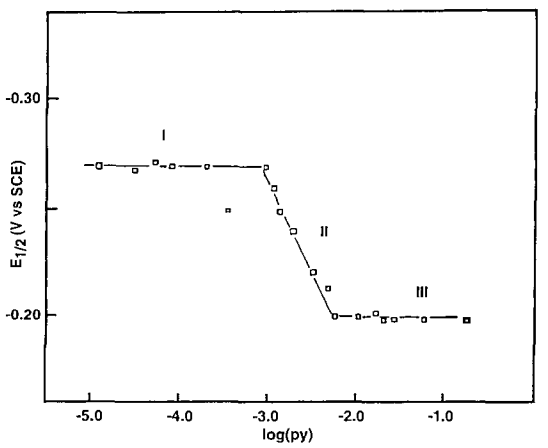

Fig. 6. Plot of $E_{1/2}$ for the Mn^{III}/Mn^{II} reaction of 10^{-3} M (TPP)Mn[$N_4C(C_6H_5)$] in CH_2Cl_2 containing 0.1 M (TBA)ClO_4 and 0.01–100 equiv. pyridine.

As mentioned above, the $E_{1/2}$ values for the first reduction of the tetrazolato complexes are virtually independent of the nature of the tetrazolato group in strongly coordinating solvents such as neat pyridine (see Table 6). The measured reduction potentials are also identical to $E_{1/2}$ values for other manganese porphyrins bearing an anionic axial ligand under the same experimental conditions.[28] Manganese(III) porphyrins of the type (P)MnX, where X = Cl^-, Br^- or I^-, undergo a loss of the halide axial ligand after electroreduction in coordinating solvents, and the same type of behaviour seems to be observed for each of the four tetrazolato manganese(III) porphyrins investigated in the present study.

Finally, it should be noted that the second and third reductions of (TPP)MnX compounds with anionic axial ligands unambiguously involve the π-ring system and this seems to also be the case for the four tetrazolato manganese complexes whose electrochemical behaviour is similar to that of (TPP)MnX under the same experimental conditions. The Mn^{II} reductions are irreversible in CH_2Cl_2 but become reversible in PhCN, THF or py.

Acknowledgement—The support of the Robert A. Welch Foundation (KMK E-680) and CNRS (RG UMR 9953) is gratefully acknowledged.

REFERENCES

1. L. J. Boucher, *Coord. Chem. Rev.* 1972, **7**, 289.
2. M. Calvin, *Rev. Pure Appl. Chem.* 1965, **15**, 1.
3. B. C. Schardt, F. J. Hollander and C. L. Hill, *J. Am. Chem. Soc.* 1982, **104**, 3964.
4. M. J. Camenzind, F. J. Hollander and C. L. Hill, *Inorg. Chem.* 1983, **22**, 3776.
5. C. L. Hill and F. J. Hollander, *J. Am. Chem. Soc.* 1982, **104**, 7318.
6. J. W. Buchler, C. Dreher, K.-L. Lay, Y. J. A. Lee and W. R. Scheidt, *Inorg. Chem.* 1983, **22**, 888.
7. J. T. Groves and M. K. Stern, *J. Am. Chem. Soc.* 1988, **110**, 8628.
8. M. Rodriguez, T. Kodadek, M. Torresand and A. J. Bard, *Bioconj. Chem.* 1990, **2**, 123.
9. R. Fawwaz, P. Bohidiewicz, D. Lavallee, T. Wang, S. Oluwole, J. Newhouse and P. Alderson, *Nucl. Med. Biol.* 1990, **17**, 65.
10. B. Meunier, *Chem. Rev.* 1992, **92**, 1411.
11. R. Huisgen, *Angew. Chem., Int. Edn Engl.* 1963, **2**, 633.
12. G. L'Abbé, *Chem. Rev.* 1969, **69**, 345.

13. S. Patai, *The Chemistry of Azido Group*. Interscience, New York (1971).
14. R. Huisgen, in 1.3-*Dipolar Cycloaddition Chemistry* (Edited by A. Padwa), Vol. I, Ch I. Interscience, New York (1984).
15. E. F. V. Scriven, *Azides and Nitrenes, Reactivity and Utility*. Academic Press, Orlando, FL (1984).
16. (a) R. Guilard, S. S. Gerges, A. Tabard, P. Richard, M. A. El Borai and C. Lecomte, *J. Am. Chem. Soc.* 1987, **109**, 7228; (b) R. Guilard, N. Jagérovic, A. Tabard, P. Richard, L. Courthaudon, A. Louati, C. Lecomte and K. M. Kadish, *Inorg. Chem.* 1991, **30**, 16; (c) R. Guilard, N. Jagérovic, A. Tabard, C. Naillon and K. M. Kadish, *J. Chem. Soc., Dalton Trans.* 1992, 1957.
17. R. Guilard, I. Perrot, A. Tabard, P. Richard, C. Lecomte, Y. H. Liu and K. M. Kadish, *Inorg. Chem.* 1991, **30**, 27.
18. N. Jagérovic, J.-M. Barbe, M. Farnier and R. Guilard, *J. Chem. Soc., Dalton Trans.* 1988, 2569.
19. K. Nakamoto, in *Infrared and Raman Spectra of Inorganic and Coordination Compounds*. John Wiley and Sons, New York (1978).
20. M. Gouterman, in *The Porphyrins* (Edited by D. Dolphin), Vol. III, p. 50. Academic Press, New York (1978).
21. G. N. La Mar and F. A. Walker, *J. Am. Chem. Soc.* 1973, **95**, 6950.
22. G. N. La Mar and F. A. Walker, *J. Am. Chem. Soc.* 1975, **97**, 5103.
23. G. C. Brackett, P. L. Richards and W. S. Caugley, *J. Chem. Phys.* 1971, **54**, 4383.
24. G. N. La Mar and F. A. Walker, in *The Porphyrins* (Edited by D. Dolphin), Vol. IV, p. 61. Academic Press, New York (1978).
25. T. R. Janson, L. J. Boucher and J. J. Katz, *Inorg. Chem.* 1973, **12**, 940.
26. K. M. Kadish, M. Sweetland and J. S. Cheng, *Inorg. Chem.* 1978, **17**, 2795.
27. S. L. Kelly and K. M. Kadish, *Inorg. Chem.* 1979, **18**, 2968.
28. S. L. Kelly and K. M. Kadish, *Inorg. Chem.* 1982, **21**, 3631.
29. R. D. Arasasingham and T. C. Bruice, *Inorg. Chem.* 1990, **29**, 1422.
30. B. M. Hoffman, C. J. Weschler and F. J. Basolo, *J. Am. Chem. Soc.* 1976, **98**, 5473.